

Contrasting rainfall behavior between the Pacific coast and the Mexican Altiplano

José Pablo Vega-Camarena^{1,*}, Luis Brito-Castillo¹, Luis M. Farfán²

¹Centro de Investigaciones Biológicas del Noroeste (CIBNOR), Guaymas, Sonora 85454, Mexico

²Centro de Investigación Científica y de Educación Superior de Ensenada (CICESE), La Paz, Baja California Sur 23050, Mexico

ABSTRACT: Summer rainfall along the coast Nayarit, Mexico, behaves in a contrasting way to rainfall observed on the Mexican Altiplano. The mechanism for this behavior originates in the wind flow and moisture content of the atmospheric column. By using field observations from 2015, this study analyzed wind and rainfall characteristics in the interior of the San Pedro-Mezquital river basin, which connects the Pacific coast and the Mexican Altiplano. At the surface, the characteristics of humidity transport that explain rainfall in one region hinder its transport to the other. This has not been previously documented. We further analyzed different scenarios with sets of daily data, using composite maps of average wind and specific humidity at 500, 700, and 1000 hPa to explain these anomalies. In 2015, a pattern resembling the midsummer drought occurred at a weather station located on the coast. The corresponding time series of precipitation, which was derived from an analysis of orthogonal empirical functions with varimax axis rotation, showed that from 1970–2012, there were 3 years (1978, 2000, and 2002) with droughts. The mechanism that caused this behavior originates in the gap in the occurrence of mesoscale convective systems (MCSs), with environmental conditions that provide more convection and enhanced rainfall in September over coastal areas. The September rainfall in these 3 years contrasts that over the Mexican Altiplano, giving more evidence of a seesaw rainfall pattern between these 2 regions.

KEY WORDS: Rainfall · Pacific coast · Mexican Altiplano · Mesoscale convective systems

Resale or republication not permitted without written consent of the publisher

1. INTRODUCTION

The distribution of summer rainfall in northwestern Mexico is largely controlled by the North American Monsoon (Ropelewski et al. 2005, Higgins & Gochis 2007). According to Turrent & Cavazos (2009), the development of the monsoon is due to the thermal contrast between the continent and the adjacent oceanic region. Rainfall in the region does not occur homogeneously, nor with consistent intensity. Gochis et al. (2004) found that the largest portion of daily rainfall occurs early in the day, and more often at the higher elevations of the Sierra Madre Occidental (SMO), but with reduced intensity. At lower elevations, precipitation is not frequent but has greater intensity (Berbery 2001). The beginning of the rain-

fall regime is initiated by abrupt changes from hot and dry weather conditions in late June to wetter and cooler conditions in early July (Higgins et al. 2003). Maximum rainfall extends gradually from south to north, along the Pacific coast to the northern edge of Arizona. In August, rainfall returns to the south and west, reaching the southern part of the Baja California peninsula.

The rainfall maximum progresses with summer, although a region between the Pacific coast and the Mexican Altiplano has a maximum rainfall pattern that is out of phase by 1 mo as summer progresses (Brito-Castillo et al. 2010). This pattern led to several studies attempting to explain the anomaly. Deep canyons through the SMO connect coastal Nayarit with the Mexican Altiplano, suggesting a dynamic

*Corresponding author: jcamarena006@gmail.com

link between the coast and the Altiplano, but this link does not explain how the moisture manages to cross the mountain barrier of the SMO, with elevations exceeding 3 km.

Brito-Castillo et al. (2010) suggest that the configuration of the San Pedro-Mezquital river system—with deep canyons and lower elevations (compared with canyons of adjacent river systems) in their upper parts that reach into the Altiplano—can help to understand the dynamics governing this rainfall system. Vega-Camarena et al. (2018) found that when rainfall is abundant in the Altiplano, there is a lack of rainfall on the coast of Nayarit, and vice versa. This seesaw structure has been reported for other regions of Mexico. For example, Méndez & Magaña (2010) suggest that when there is a reduction in rainfall as a negative anomaly in southeastern Mexico, there is a positive rainfall anomaly in northern Mexico, and vice versa; however, the mechanism governing this pattern is different than that mentioned by Vega-Camarena et al. (2018).

A major source of rainfall along the coast of Nayarit are mesoscale convective systems (MCSs) that develop between July and September. These MCSs modulate the spatial and seasonal variability of summer rainfall patterns of the monsoon (Farfán & Zehnder 1994). An MCS is an organized cluster of clouds that provides a contiguous area of precipitation, ranging over 100 km (Houze 1993), with a lifecycle of several hours (Zipser 1982). In northwestern Mexico, MCSs initially develop over the higher elevations and move to the coast, reach their maximum extent along the coast, and dissipate over the Gulf of California. According to Howard & Maddox (1988), MCSs have an average lifetime of 15 h. Valdés-Manzanilla et al. (2005) state that MCSs initiate at dusk and dissipate near midnight. Although the characteristics of deep convection have been documented by geostationary satellites (Purdum 1976, Velasco & Fritsch 1987), little is known about the different types of MCSs that develop in western Mexico. Another important source of moisture in this region are tropical cyclones that provide large amounts of rain, especially in Sinaloa, Durango, Nayarit, and Jalisco (Farfán et al. 2013, Martínez-Sánchez & Cavazos 2014). Tropical cyclones have more influence on Mexican rainfall in September at their maximal northeast extent in the eastern Pacific. Additionally, easterly waves crossing the Atlantic to the eastern Pacific, associated with a strong vertical coupling from adiabatic heating, influence precipitation patterns over western Mexico (Giovannetone & Barros 2008, Ladwig & Stensrud 2009).

Our goal was to document the behavior of rainfall observed between the coast of Nayarit and the Mexican Altiplano. For this purpose, we analyzed the atmospheric moisture content at 1000 hPa, 700 hPa, and 500 hPa, as well as the behavior of winds and rain inside the San Pedro-Mezquital river system, where no conventional weather stations are available. Here, we installed 4 automatic meteorological stations (Vantage Vue, Davis). Thus, this study is the first effort to document wind and rain measurements inside the river system. Our goal was (1) to understand the low-level dynamics and rainfall when the seesaw structure appears between the coast of Nayarit and the Altiplano, and (2) to document whether there is a rainfall pattern resembling the midsummer drought along coastal Nayarit. The midsummer drought is defined as a temporary reduction of precipitation during July and August, causing a bimodal distribution of rain with maxima during June and September–October. Since rainfall distribution at these latitudes is dominated by the monsoon circulation, which is characterized by one rainfall maximum during the warm season, the causes of the midsummer drought along coastal Nayarit are expected to be different from those proposed by Mosiño & García (1974), Magaña et al. (1999), and Karnauskas et al. (2013).

2. DATA AND METHODS

2.1. Study area

The San Pedro-Mezquital river system (Fig. 1) contains 3 main tributaries and crosses the Mexican Altiplano through the Mezquital canyon. It then crosses the mountains to the southwest and irrigates the valleys of Ruiz, Nayarit, ending at Marismas Nacionales, an extensive coastal wetland (CONANP 2013), after covering a distance of 540 km. The river system's drainage basin covers an area of 28 000 km². The upper river basin, located in the Altiplano, has a semi-arid, subtropical climate with a rainy season from June through October and annual precipitation of 500 mm.

The coast of Nayarit, unlike the Mexican Altiplano, has warm and humid conditions with annual rainfall above 1000 mm. This region has prolific MCS development between June and September, predominantly in August, which is the month with the highest rainfall (Brito-Castillo et al. 2010). Therefore, organized convection is likely to be the main source of weather events in this region.

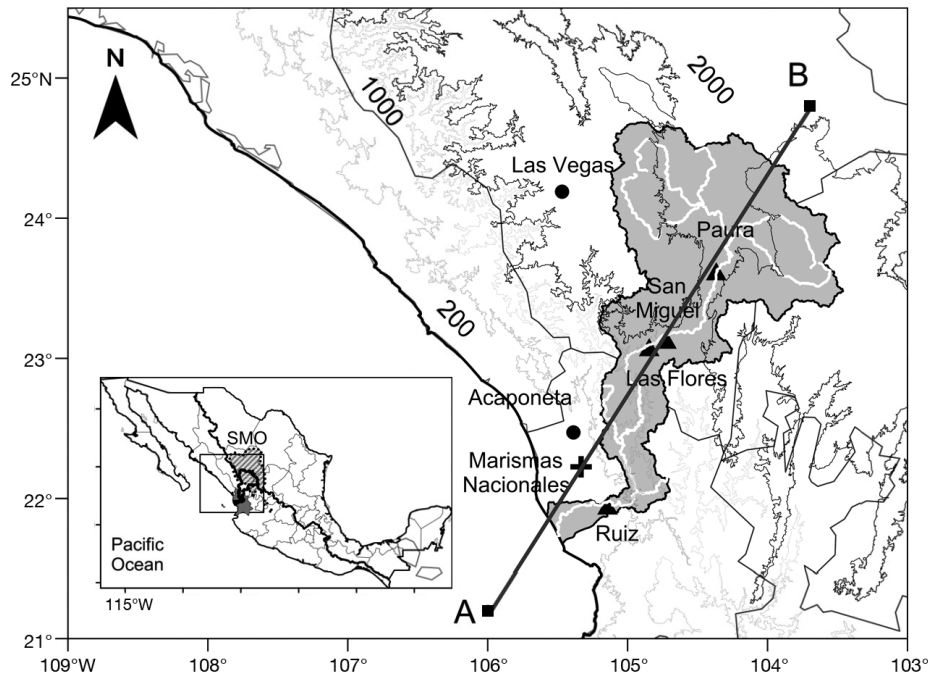


Fig. 1. Study area and geographical locations. Thick line and grey shading: basin of the San Pedro-Mezquital river; white line: river and tributaries; dots: weather stations; triangles: automated weather stations (Vantage Vue); grey contours: elevation (m); line A–B: cross section for Fig. 12. Inset shows location in western Mexico (dark grey shading: Nayarit; hatching: Altiplano). SMO: Sierra Madre Occidental

2.2. Data

Hourly observations of precipitation and wind speed and direction come from 2 automated weather stations, Acaponeta and Las Vegas (see Fig. 1) that are part of a network operated by the National Meteorological Service of Mexico. Additionally, we used 4 Vantage Vue (Davis) weather stations (www.davis-net.com/solution/vantage-vue) that store temperature, humidity, pressure, rainfall, wind speed, and wind direction data.

The additional stations were installed within the basin, considering the following criteria: (1) elevation of the site; (2) sites where conventional meteorological stations were not available; (3) accessibility of the site; (4) a distance of >5 km between the nearest settlement and the main river; and (5) adequate conditions for each station to record the variables of interest. Thus, the communities chosen for the installation of the stations were Paura, Las Flores, and San Miguel within the San Pedro-Mezquital river drainage area, and at Ruiz near the Pacific coast (Fig. 1).

Data were recorded from 1 July through 30 September 2015. All precipitation records had complete hourly data during this period, except Ruiz which provided only $\sim 98.0\%$ of its records due to temporary interruptions. At Ruiz, missing data occurred in short

periods of 3 h: 1 in July, 1 in August, and 1 in September 2015. All records were subject to data quality analysis that removed suspicious data, i.e. values with hourly magnitudes much higher than the range of variability of the series and which were not repeated at the other stations. For example, records were discarded if rainfall was >150 mm h^{-1} and wind speed was >11.0 m s^{-1} in Acaponeta, and if rainfall was >20 mm h^{-1} and wind speed was >11.0 m s^{-1} in Las Vegas. The rain and wind records of the remaining stations showed no suspicious data.

Additionally, we used the longest series from the National Meteorological Service through the Climate Computing Project (Zillman 2009), for the period 1920–2017. Data quality was verified before calculations through direct inspection of each series. When an individual record was found to be extremely high or extremely low, without replication in surrounding stations, the record was considered a gap. Negative values were removed from precipitation records and replaced by gaps. The monthly precipitation sums for each station were computed from daily precipitation sums. As Fig. S1 in the Supplement at www.int-res.com/articles/suppl/c076p225_supp.pdf shows, no conventional weather stations were located in the middle of the San Pedro-Mezquital river basin.

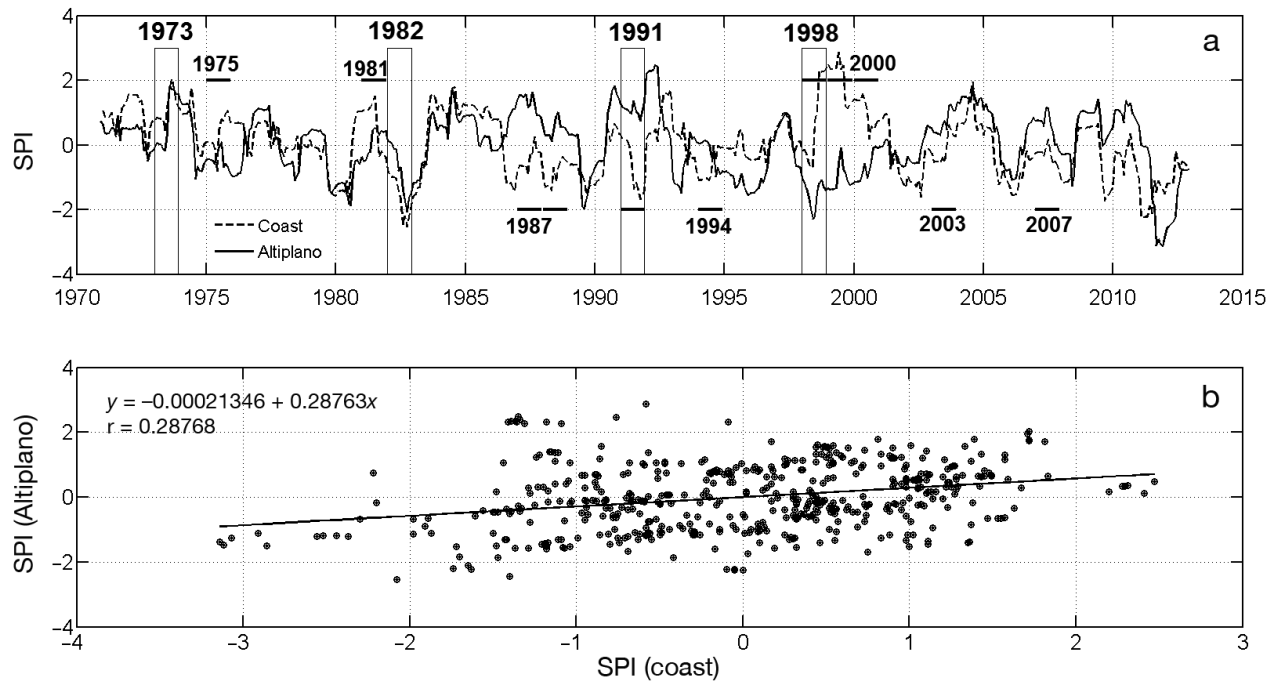


Fig. 2. (a) Standardized precipitation index (SPI) series at 12 mo scale for the Pacific coast and the Altiplano and (b) its regression line. The bold lines in (a) show the years when the rainfall seesaw between the coast and the Altiplano is evident while the bars display the years in the 12 mo scale when different relationships between the coast and the Altiplano occur

To complete the climatological analysis at the regional level, we use the standardized precipitation index series for 12 mo (SPI-12; McKee et al. 1993) for the coast and the Altiplano. These series were plotted for the period 1970–2012 (Fig. 2). Monthly mean regional series for the coast and the Altiplano were derived based on empirical orthogonal functional analysis, using the method of North et al. (1982) and Varimax-axis rotation (see details in Vega-Camarena et al. 2018). As shown in Fig. 2, the rainfall seesaw between the coast and the Altiplano appears irregularly throughout the period, which is indicative of the non-linear nature of rainfall fluctuations (Fig. 2a). Different relationships between both series are evident. For example, above-average rainfall (i.e. wet conditions) at the coast vs. below-average rainfall (i.e. dry conditions) in the Altiplano (as in 1975, 1981, 1998, 1999, and 2000), or vice versa: dry at the coast vs. wet in the Altiplano (1987, 1988, 1991, 1994, 2004, and 2007). The Pearson correlation between the series, though small ($r = 0.29$), is statistically significant ($p < 0.05$, Fig. 2b). This result indicates that the rainfall seesaw between the coast and the Altiplano is not the only possible relationship. Other relationships such as wet–wet (1973 and others) or dry–dry (1982 and others) are also possible. Fig. 3 displays the monthly mean total precipitation for the coastal region for the period 1970–2012. A single maximum is evident in all

years, except in 1978, 1982, 1987, 1998, 2000, and 2002, when unusual bimodal precipitation distribution occurred, resembling the midsummer drought. This behaviour is unusual, since the climatology of the region indicates one single precipitation peak. A single peak indicates that precipitation in the region is, in large part, controlled by the North American Monsoon system. Usually the peak is observed in August, as is discussed in Brito-Castillo et al. (2010).

2.3. Climatology

Table 1 shows the cumulative seasonal rainfall from 1 July through 30 September 2015 and monthly observations at the stations considered in this study as well as their corresponding climatology (1951–2010). The seasonal rainfall at Acajoneta and Las Vegas was compared with long-term climatology to classify summers as dry, wet, or normal. For the other stations shown in Table 1, it was not possible to perform this analysis because they provide data only for the summer of 2015, and no conventional weather stations were available in their region. The climatology was derived from nearby stations, and is available online (<https://smn.cna.gob.mx/es/climatologia/informacion-climatologica>). The analysis is corroborated by long-term observations in the surrounding area (see Fig. S1).

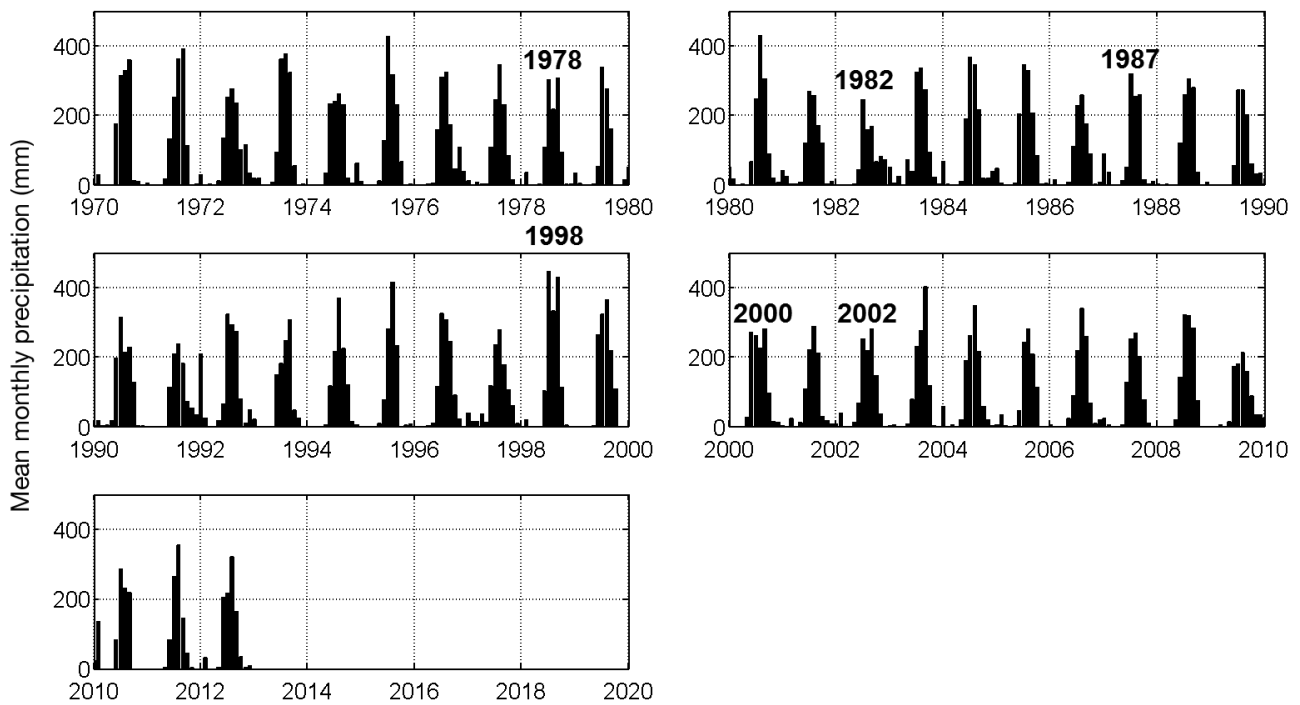


Fig. 3. Monthly mean total precipitation derived from weather stations of the coast region after applying the empirical orthogonal functional analysis for the period 1970–2012. The years with the occurrence of the uncommon midsummer drought are indicated in each plot

2.4. Rainfall and wind distribution

Fig. 4 shows accumulated, time-averaged rainfall for each station and its corresponding average wind cycle under wet conditions (i.e. rainfall > 0 mm). We consider a daily cycle to take place between 19:00 h UTC (13:00 h local time) and 18:00 h UTC (12:00 h) the following day. Within this period, all stations recorded rainfall. At San Miguel and Las Flores, in the mountain area of the San Pedro-Mezquital river basin, the occurrence of rainfall began at noon (19:00 h UTC, 13:00 h local time), while at Acaponeta, near the coast, the records started later (22:00 h

UTC, 16:00 h local time). In most cases, the rainfall continues until the next morning. This way, the day of the year of 24 h accumulation corresponds to the cycle that ends at 18:00 h UTC throughout the study area. Fig. 5 shows the series of daily accumulated rainfall between 1 July (Day 182) and 30 September (Day 273). In this period, days with no rainfall were identified at each station and the wind cycle was averaged for these days (i.e. dry conditions; Fig. 6) to contrast the characteristics of dry and wet conditions (Fig. 6 vs. Fig. 4). Time series of monthly precipitation for the coast and the Altiplano are shown in Fig. 7.

Table 1. Comparison between the accumulated summer (July–September) and monthly accumulated precipitation (mm) in 2015, with its respective mean annual precipitation for the 1951–2010 period (i.e. climatology). NA: not available; Clim: climatology; *conventional weather station; +installed automatic weather station

Station	Elevation (m)	July		August		September		Summer	
		2015	Clim	2015	Clim	2015	Clim	2015	Clim
Acaponeta*	24	229	351	184	372	517	319	930	1042
Las Vegas*	1391	192	176	116	169	110	148	418	493
Paura+	1483	160	NA	71	NA	77	NA	308	NA
Las Flores+	2180	199	NA	230	NA	158	NA	587	NA
San Miguel+	1847	181	NA	135	NA	234	NA	550	NA
Ruiz+	28	278	NA	411	NA	569	NA	1258	NA

2.5. Composite maps

Using daily data of the National Centers for Environmental Prediction–National Center for Atmospheric Research (NCEP–NCAR; Kalnay et al. 1996), composite maps of wind and specific humidity were constructed for 500, 700, and 1000 hPa. They were averaged for each month: (1 to 31 July; 1 to 31 August; and 1 to 30 September). Data for

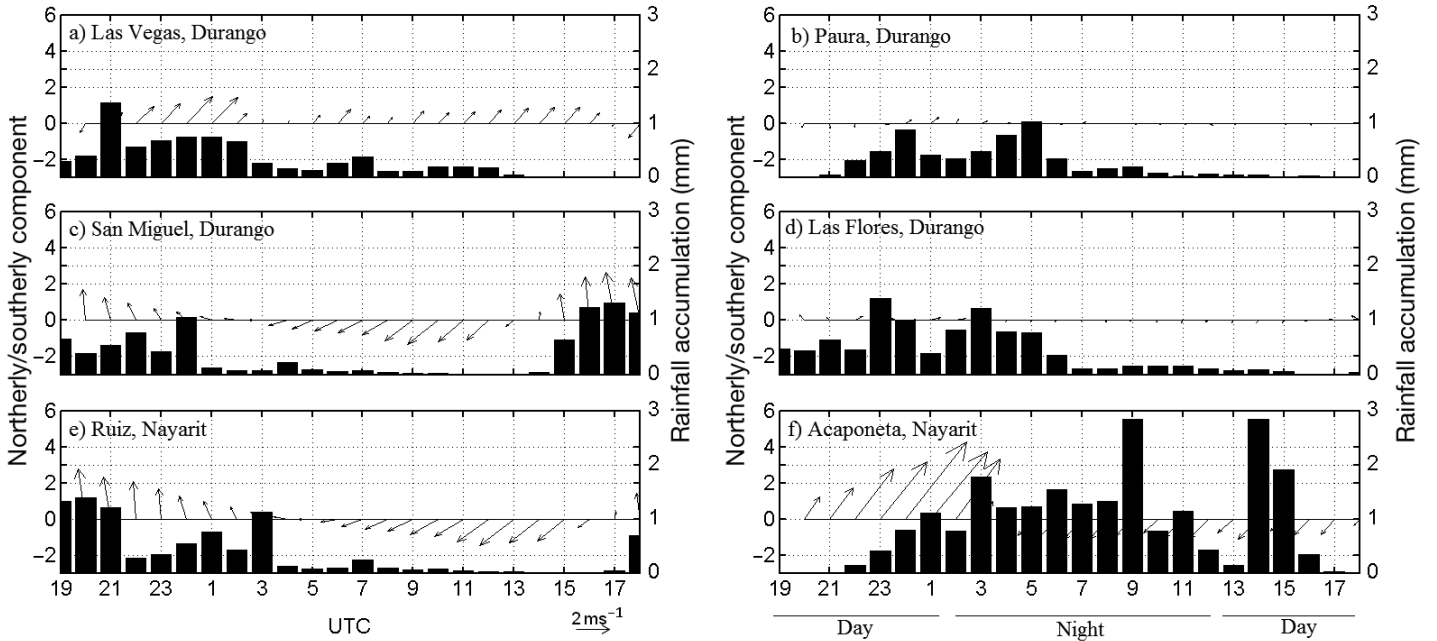


Fig. 4. Average rainfall accumulation and wind vectors at hourly intervals from 1 July through 30 September 2015

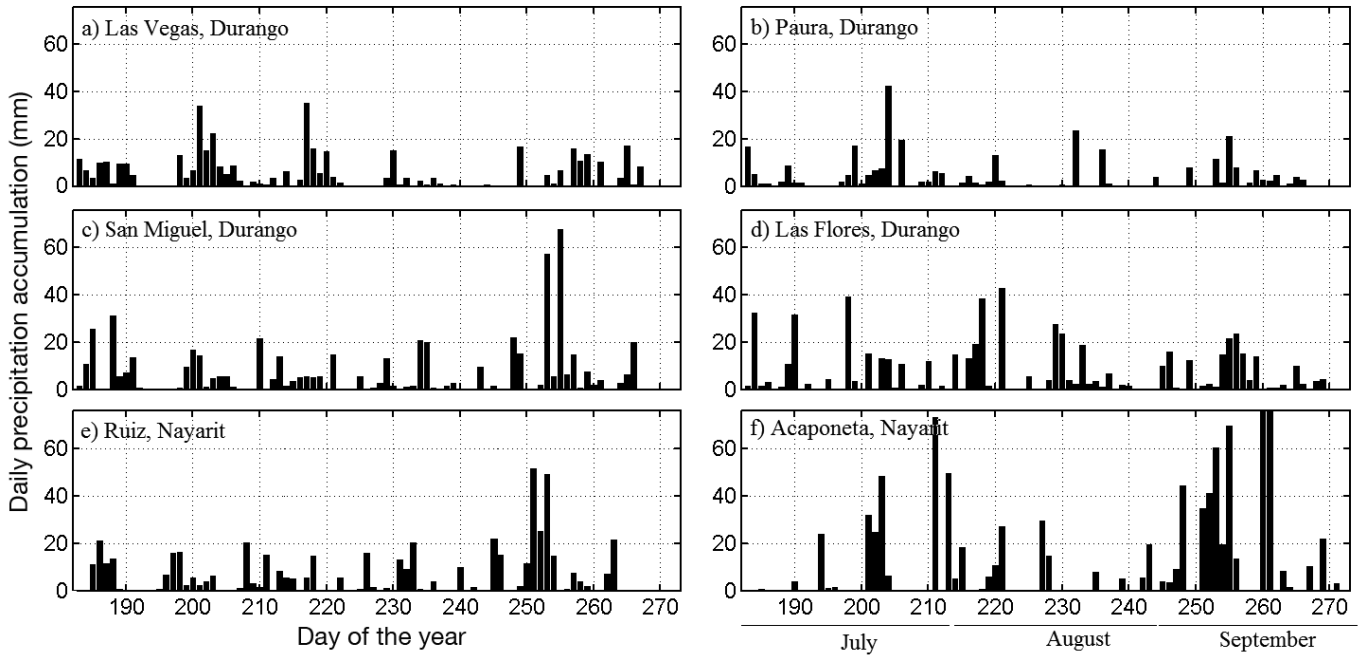


Fig. 5. Time series of daily precipitation accumulation between 1 July (Day 182) and 30 September (Day 273) of 2015

these maps were provided by the NOAA/ESRL Physical Sciences Division, available at www.esrl.noaa.gov/psd/cgi-bin/data/composites/printpage.pl. Data from the North American Regional Reanalysis (NARR; Mesinger et al. 2006) was used to build a set vertical profiles to better understand 3D structures.

2.6. Mesoscale Convective Systems (MCSs)

Identification of MCSs between July and September 2015 used digital infrared imagery from GOES-15 with 4 km spatial resolution, following the methodology of Farfán & Zehnder (1994). Additionally, the

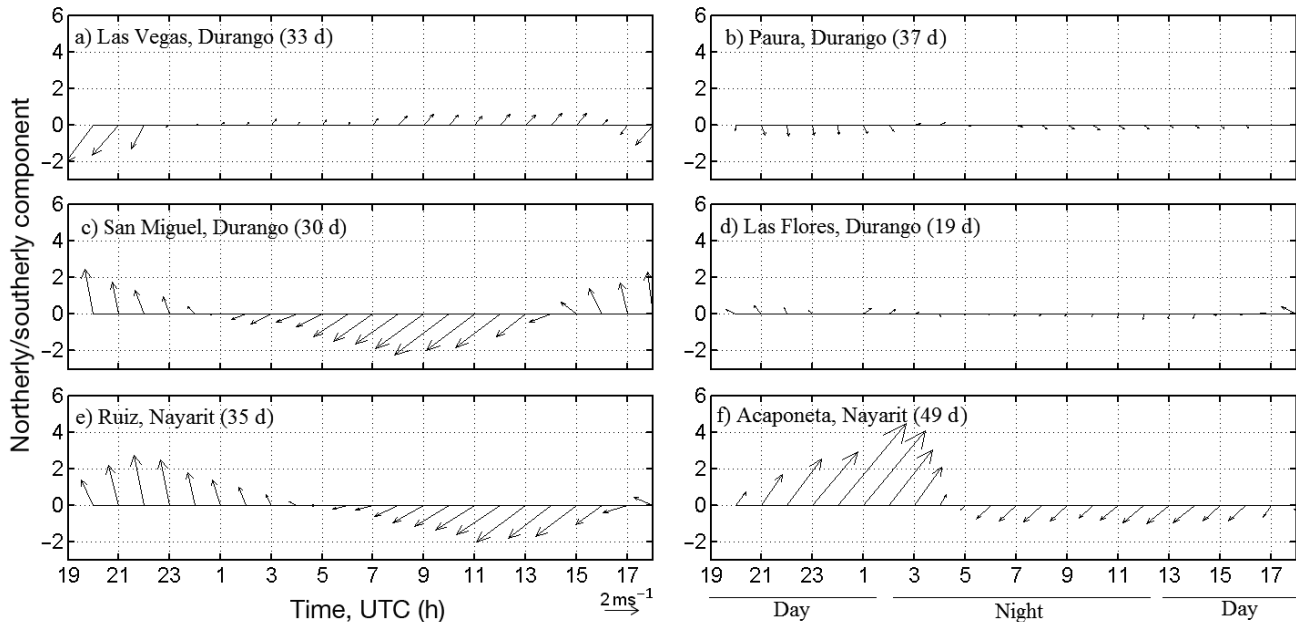


Fig. 6. Average winds for days with no rainfall between July and September 2015. For each day, the diurnal cycle begins at 19:00 h UTC and ends at 18:00 h UTC the following day

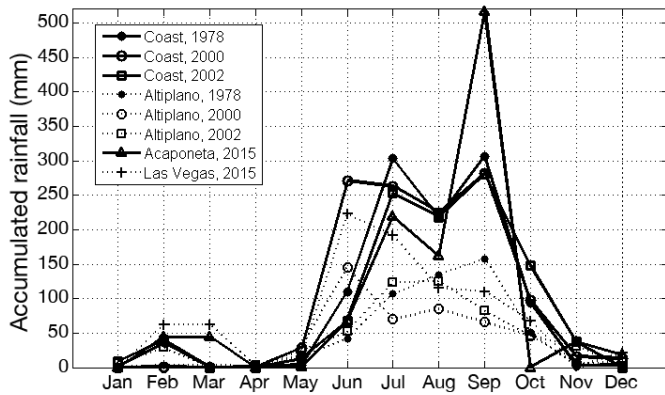


Fig. 7. Accumulated monthly rainfall for the regional series of the coast (solid lines) and the Altiplano (dotted lines) in 1978 (●), 2000 (○), and 2002 (□), at Acaponeta (Δ), and Las Vegas (+)

accumulated precipitation time of occurrence associated with each MCS and an assignment of moisture sources is based on 6 hourly tropical surface analyses available from the National Hurricane Center at www.nhc.noaa.gov/tafb.

3. RESULTS

3.1. Seasonal analysis of precipitation

Data from Acaponeta and Las Vegas show that cumulative rainfall from July to September 2015 was lower than their respective mean summer (Jul–Sep)

precipitation for the 1951–2010 period (Table 1). That is, 930 mm vs. 1042 mm at Acaponeta and 418 mm vs. 493 mm at Las Vegas. This indicates that rainfall in summer 2015 was below the long-term average. This agrees with the report issued by the National Meteorological Service, showing that our study region was generally dry during the summer of 2015 (CONAGUA 2015).

Monthly analyses in 2015 show different conditions throughout the summer, depending on the station location. In July, for example, rainfall at Acaponeta (229 mm), near the coast, was less than the mean accumulation (351 mm) based on the 1951–2010 period, while Las Vegas, located inland, received 192 mm, more than the usual 176 mm. The behavior was reversed in September, with 517 mm vs. 319 mm at Acaponeta and 110 mm vs. 148 mm at Las Vegas. In August, precipitation was lower at both stations (Table 1). For the entire region, monthly precipitation anomaly contours for 2015 were built with stations that had >30 yr of records (Fig. S2 in the Supplement). In July, negative contours (i.e. below long-term average precipitation) dominated near the coast, while positive contours (above average precipitation) covered a band across the middle of the San Pedro-Mezquital basin and a large portion of the Altiplano (Fig. S2a), indicative of the seesaw precipitation pattern between the coast and the Altiplano. In August, below-average precipitation predominated in the entire area, except in the southeast of the Altiplano (Fig. S2b), indicating that drought conditions

in August were prevalent. In September, positive (negative) contour anomalies were evident near the coast (in the Altiplano), displaying again the seesaw precipitation pattern between both regions but in opposite configuration compared to July (Fig. S2c). Finally, total precipitation contour anomalies for summer (July–September), 2015 were below average, a result that agrees with the report of the National Meteorological Service (CONAGUA 2015) and the analysis of individual stations (Fig. S2d). Based on these results, we analyzed the contrasting behavior of increased rainfall in July and September and rainfall scarcity in August. We extrapolated these results to the whole region to identify the physical causes. From July to September, MCSs develop on the coast of Nayarit (Howard & Maddox 1988), which supply significant amounts of rainfall. These systems are more active in August and modulate the seasonal patterns of accumulated rainfall from the monsoon, not only at the coast, but also in the inland region. This is mainly derived from the warm waters of the Gulf of California and the topography, as suggested by Brito-Castillo et al. (2010). This is why the rainfall maximum usually occurs in August; however, in other areas where the monsoon circulation predominates, the rainfall peak tends to be in July. Our study area also receives rainfall contributions from tropical cyclones, but these are mainly in September, when they reach their highest northward displacement (CENAPRED 2014).

The summer of 2015 lacked rainfall in the study area, a condition that is consistent with limited accumulations in August. In July and September, a seesaw behavior occurred, with opposing conditions between Acaponeta and Las Vegas. Another characteristic of the rainfall pattern was that it had a bimodal form in Acaponeta (Fig. 8), with a peak in July and a higher peak in September, and with a decline in August that resembled the midsummer drought (Mosiño & García 1974, Magaña et al. 1999) that occurs in southeastern Mexico. In the study area, the monsoon circulation is characterized by a single maximum, which is not consistent with the explanation given by Karnauskas et al. (2013) for the midsummer drought. The Florida, Paura, and San Miguel stations had a similar pattern of midsummer drought in 2015, although with a less pronounced peak in September. As in 2015, the rainfall along the coast resembled the midsummer droughts in 1978, 2000, and 2002, with the highest peak in September (Fig. 7). These characteristics are useful to contrast the conditions observed in 1978, 2000, and 2002 relative to 2015. Since there are observations from the San Pedro-Mezquital basin, we pro-

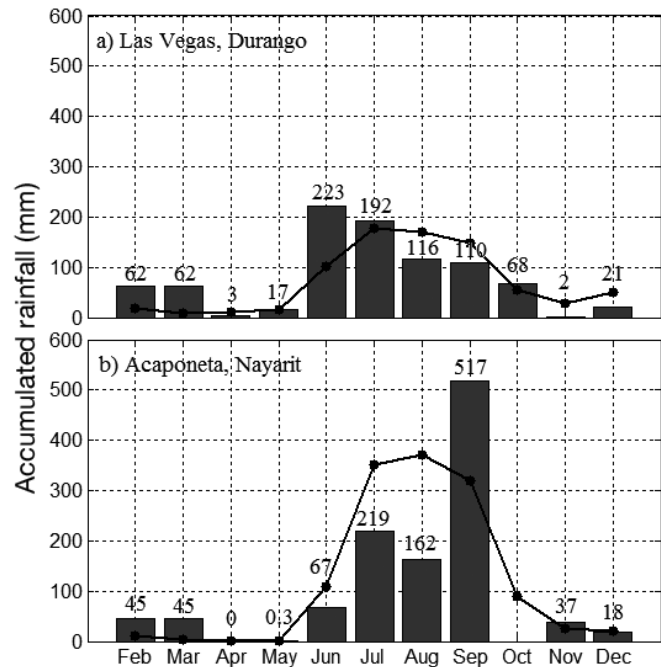


Fig. 8. Accumulated monthly rainfall (bars) in 2015 for (a) Las Vegas, and (b) Acaponeta. The line represents the 1951–2010 mean monthly precipitation

vide an explanation of the conditions that give rise to the midsummer drought in those years. Other years that showed the uncommon midsummer drought in the coastal region, but with the highest peak in July are 1982, 1987, and 1998 (see Fig. 3). In the summers of 2000 and 2002, rainfall patterns were reversed in the 2 regions (Fig. 7).

3.2. Flow patterns

Average wind and specific humidity at 500, 700, and 1000 hPa were computed for July, August, and September 2015 (Fig. 9). In July (Fig. 9a–c), at 500 hPa, humid conditions over the continent included a plume of moisture from the tropical Pacific moving into northwestern Mexico and the southwestern United States. The plume grew, along with a weak east-southeast flow. At 700 hPa, the highest concentration of moisture was located over northwestern Mexico, although smaller amounts also covered the upper part of the San Pedro-Mezquital river basin. At this level, easterly winds crossing the continent in the tropics were more intense. Low-level (1000 hPa) moisture was present over central and southern Mexico, covering the entire basin. At this level, strong easterly winds advected moisture from the tropical Atlantic, but they weakened over the

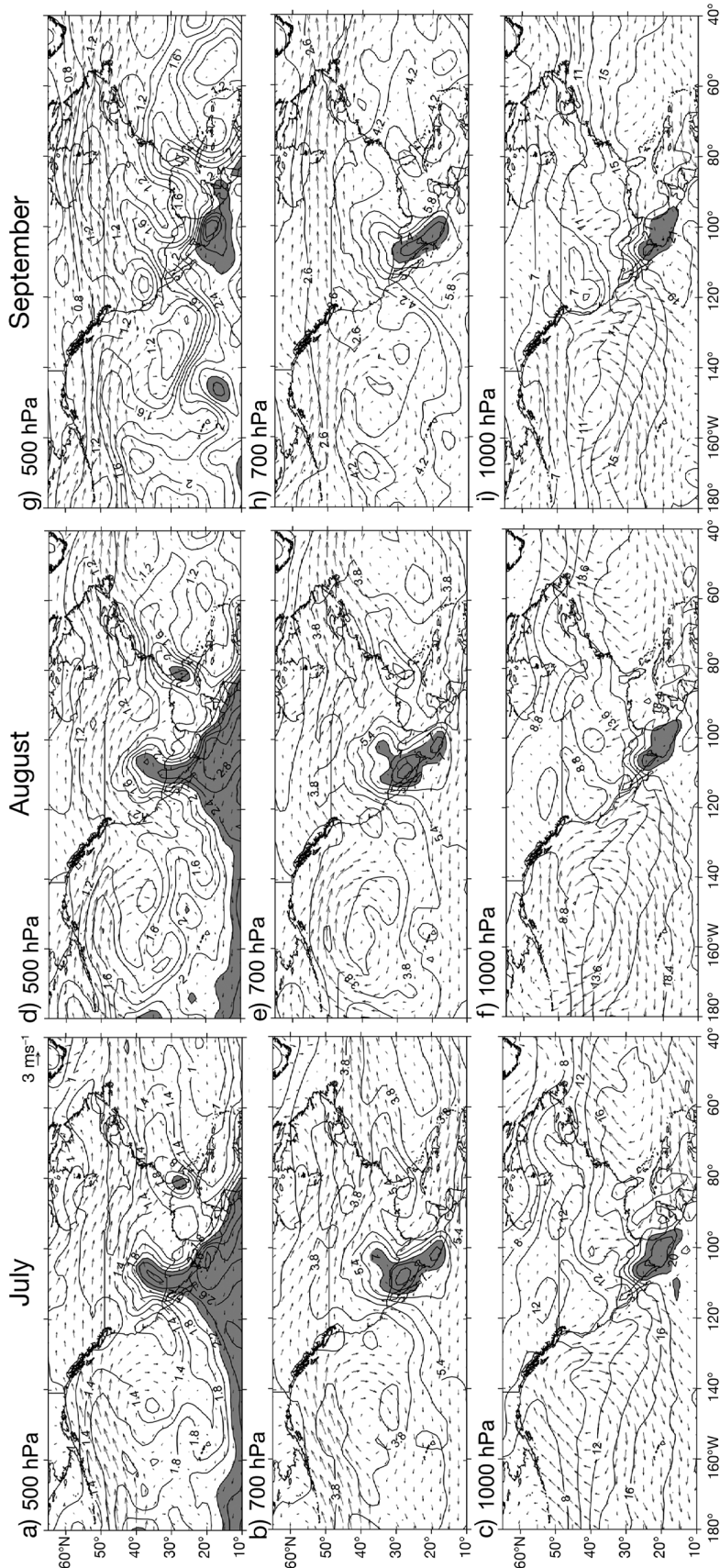


Fig. 9. Average wind vectors and specific humidity (SH, g kg^{-1} , contours), at 500 hPa, 700 hPa, and 1000 hPa in July (a–c), August (d–f) and September (g–i) 2015. Shaded area indicates $\text{SH} \geq 2.0 \text{ g kg}^{-1}$ at 500 hPa, $\text{SH} \geq 7.0 \text{ g kg}^{-1}$ at 700 hPa, and $\text{SH} \geq 20 \text{ g kg}^{-1}$ at 1000 hPa for every month

eastern Pacific and were much weaker than at 700 hPa and 500 hPa.

Humidity and wind along the Pacific and inland during August (Fig. 9d–f) had a pattern that was similar to the July distribution, with the difference that the atmospheric moisture content was lower in August.

In September (Fig. 9g–i), the distribution of moisture on the continent was different from the pattern in July and August. At 500 hPa, for example, the highest concentration of moisture occurred in southern Mexico, decreasing its extent at 1000 hPa, but with higher amounts over the San Pedro-Mezquital river basin. At the 1000 hPa level, there was a cyclonic circulation over the west coast of Mexico that, although it was weak, may have been related to the increase of convective activity in Nayarit. This is explored in Section 3.3. At 700 hPa, more moisture (compared to the 500 and 700 hPa levels) occurred over the central part of Mexico.

3.3. Convective activity

Fig. 10 shows a sequence of 3 hourly infrared images for September 17, 2015, when heavy rainfall was associated with an MCS (Table 2). The MCS started at 03:00 h UTC (21:00 h local time), intensified between 06:00–15:00 h UTC (00:00–09:00 h local time), and dissipated after 18:00 h UTC (12:00 h local time). This was an example of an MCS developing over land (Nayarit) before midnight and dissipating the next day, several hundred kilometers off the coast.

During the summer we identified 18 MCSs, which are listed in Table 2. September was the most prolific month with 12 MCSs, while July and August had 3 each, mainly along the coast of Nayarit. The frequency of MCSs was higher in September compared to August, which is consistent with findings displayed in Fig. 9 and Table 2, and which explains why

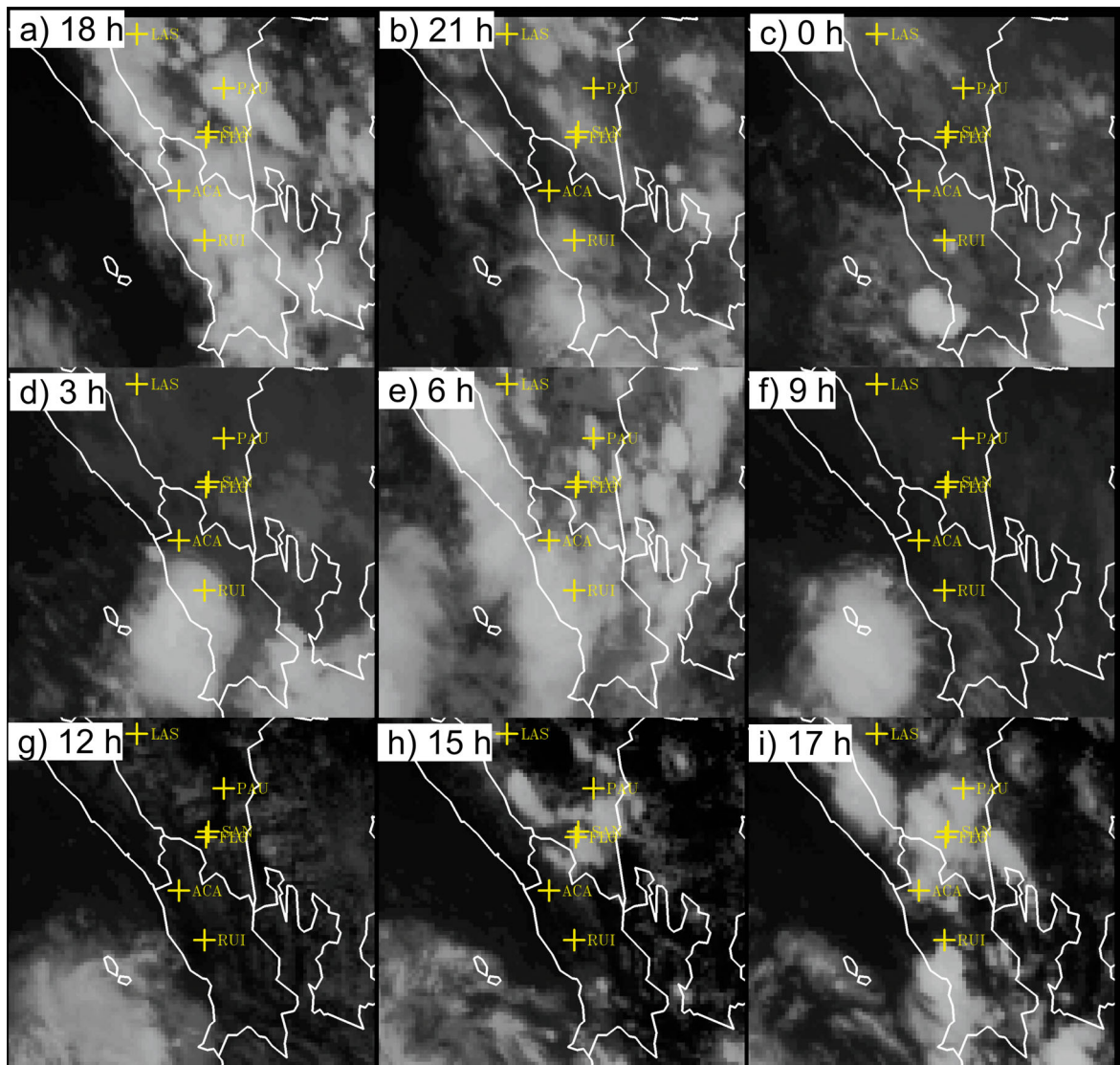


Fig. 10. Sequence of infrared images from GOES-15, beginning at 18:00 h local time (00:00 h UTC) on 16 September and ending at 17:00 h local time (23:00 h UTC) on 17 September 2015. Panels (d–f) show the development of a mesoscale convective system. +: automatic weather stations; RUI: Ruiz; ACA: Acaponeta; FLO: Las Flores; SAN: San Miguel; PAU: Paura; LAS: Las Vegas

the maximum rainfall along the coast occurs in September rather than in August, as indicated by climatology.

3.4. Surface winds

On rainy days (Fig. 4), surface winds showed a well-defined change in direction from southwest to northeast at Acaponeta (Fig. 4f) and from northeast to southwest at Las Vegas (Fig. 4a). The change occurred at 04:00 h UTC in Acaponeta and at 17:00–18:00 h UTC in Las Vegas. Acaponeta's rainfall in the evening was related to winds that blew mainly from

the northeast, while the rainfall at Las Vegas occurred in the afternoon, with winds from the southwest. Inside the San Pedro-Mezquital river basin (Paura, San Miguel, Las Flores, and Ruiz), the afternoon rainfall was linked to winds with a southward component. When winds have a northward component, it does not rain in the interior or the rainfall is modest.

On days with no rainfall, the change in wind direction resembled the above pattern but was better defined. That is, the relatively strong southwesterly winds changed to weaker northeasterly winds in Acaponeta (Fig. 6f), while in Las Vegas, strong northeasterly winds changed to weaker southwesterly winds (Fig. 6a).

Table 2. List of days in which the occurrence of mesoscale convective systems (MCSs) was identified in summer 2015 in the coastal region of the study area; rainfall accumulation in ~24 h between 18:00 h UTC and 17:30 h UTC the following day; and the thermodynamic source of humidity associated with each event. NA: not available

List	Day	Accumulated rainfall (mm 24 h ⁻¹)	Thermodynamic source
July			
1	12–13	16	Tropical cyclone
2	19–20	14	Easterly wave
3	30–31	78	Easterly wave
August			
1	02–03	43	Easterly wave
2	14–15	58	Weak cyclone
3	30–31	30	Easterly wave
September			
1	04–05	21	Easterly wave
2	07–08	20	Tropical cyclone
3	09–10	78	Easterly wave
4	10–11	75	NA
5	11–12	54	NA
6	15–16	25	Easterly wave
7	16–17	105	Easterly wave
8	17–18	112	Weak cyclone
9	19–20	29	Weak cyclone
10	22–23	37	Easterly wave
11	23–24	16	Easterly wave
12	24–25	53	Easterly wave

This pattern was confirmed, since observations showed weak winds from the northeast–northwest, which could include periods of calm and which matched rainfall (i.e. rainfall was weak when wind was calm) in San Miguel, Las Flores, Paura, and Ruiz (Fig. 6); days with no rain had northeasterly winds that were relatively strong, as seen, for example, at San Miguel and Ruiz.

To explain differences in the rainfall behavior observed within and outside the river basin, the average daily cycle between months were compared (Fig. 11). There were marked differences in rainfall accumulation and time of occurrence, with rainfall appearing earlier at inland locations. At Las Vegas, for example, rainfall in August and September occurred between 19:00 and 11:00 h UTC, while at Acaponeta rainfall occurred in August between 22:00 and 17:00 h UTC and in September between 00:00 and 15:00 h UTC. Acaponeta, unlike Las Vegas, had its maximum precipitation in the September mornings.

Inland at Paura, located in the Altiplano at the top of the basin, August and September rains came late in the day, between 22:00 and 05:00 h UTC; at Las Flores and San Miguel, located in the mountains in the middle of the basin, rainfall came earlier, starting

at 19:00 h and ending at 18:00 h UTC the next day, with a dry period between 11:00 and 15:00 h UTC. Maximum precipitation occurred between 19:00 and 00:00 h UTC in Las Flores and between 18:00 and 00:00 h UTC in San Miguel. At Ruiz, near the coast, rainfall occurred between 19:00 and 14:00 h UTC in August and between 19:00 and 09:00 h UTC in September.

Vertical profiles of the flow winds and mixing ratios for July–September, along the San Pedro-Mezquital River basin, are shown in Fig. 12. Mixing ratios in all cases displayed similar values with low-level maxima close to the coast while inland, over the Altiplano, there was lower moisture content. Wind vectors above the 700 hPa level (or 3 km approximately) were from the east (Fig. 12a) or from the E–NE (Fig. 12b–c), the mid-level flow was from the mainland toward the Pacific coast, and was linked to low mixing ratios. The most conspicuous changes in wind vectors were between the surface and 800 hPa (2 km). In July for example (Fig. 12a), in the coastal foothills, the wind came from W–NW close to the surface and from W–SW above 800 hPa. Note that the peak of the continental divide is indicated by the open arrows in Figs. 12 a–c, and a cross section (A–B) through the San Pedro-Mezquital basin is shown in Fig. 1.

Winds in the Pacific foothills yielded low-level divergence in the surface–800 hPa layer and convergence above 700 hPa (Fig. 12a). Low-level divergence implies moisture being transported to the continental divide through the San Pedro-Mezquital basin. In contrast, there was a pattern of convergence over the divide and divergence at middle levels (Fig. 12a) which was consistent with more rainfall over the Altiplano in July. In September (Fig. 12c), the configuration of low-level convergence and divergence above the divide resembled August (Fig. 12b), resulting in below-average rainfalls in the Altiplano. In contrast, September had 800–550 hPa convergence near the coast that combined with upper-level (above 500 hPa) divergence and outflow favorable for deep convection. Hence, a divergence–convergence configuration on the Pacific foothills explains the seesaw rainfall behavior between the coast and the Altiplano.

4. DISCUSSION

At the national level (CONAGUA 2015), July 2015 precipitation was 21.5% below the 1941–2014 average and was classified as the tenth-driest month. Areas where the 2015 rainfall exceeded the average were the Baja California peninsula and central Mex-

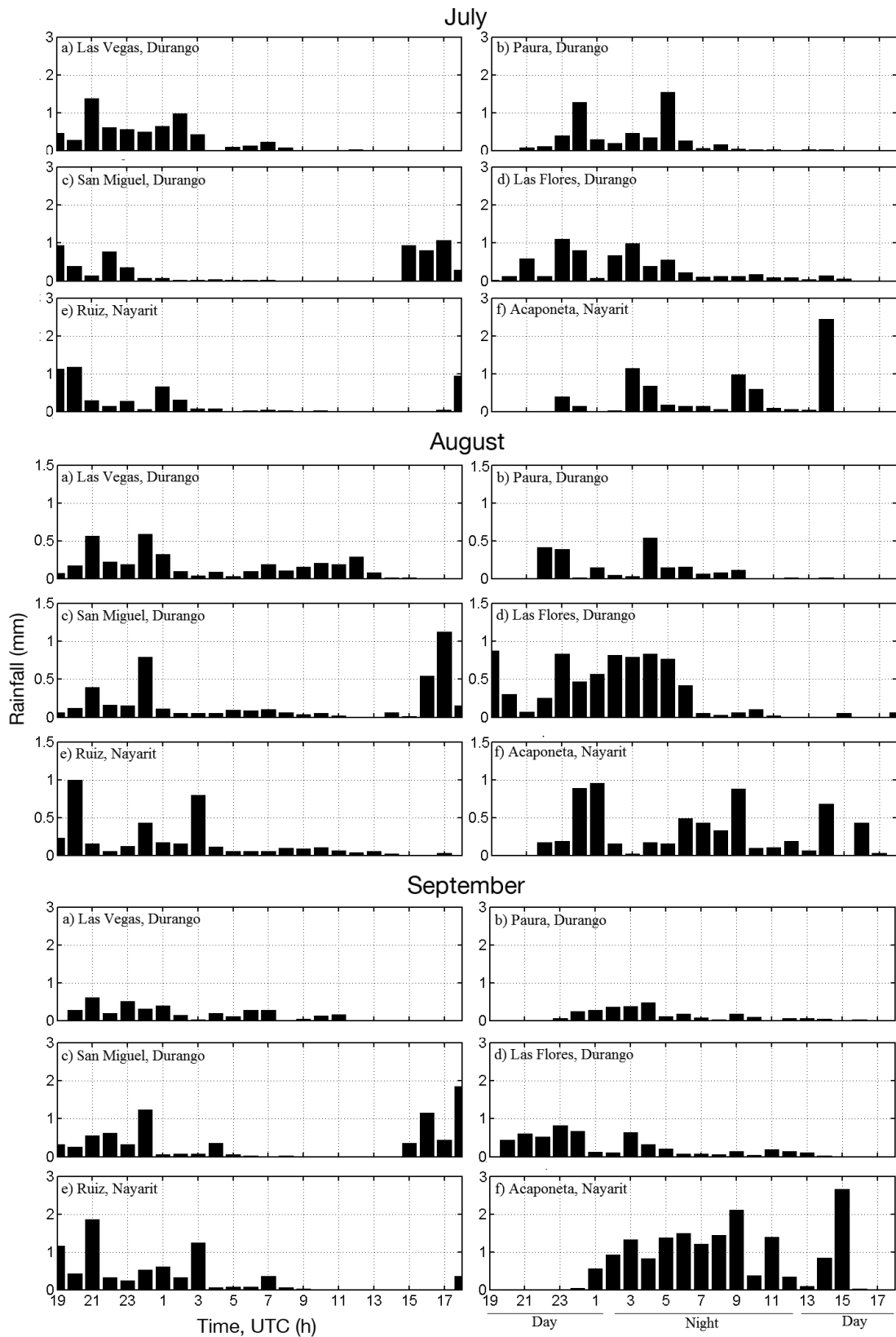


Fig. 11. Average hourly rain (mm) for July, August, and September 2015 at 6 weather stations in the study area. Initial hour is 19:00 h UTC and end is at 18:00 h UTC the following day. Ruiz and Acaponeta are located on the coast. Las Vegas, Paura, Las Flores, and San Miguel are located on the Mexican Altiplano

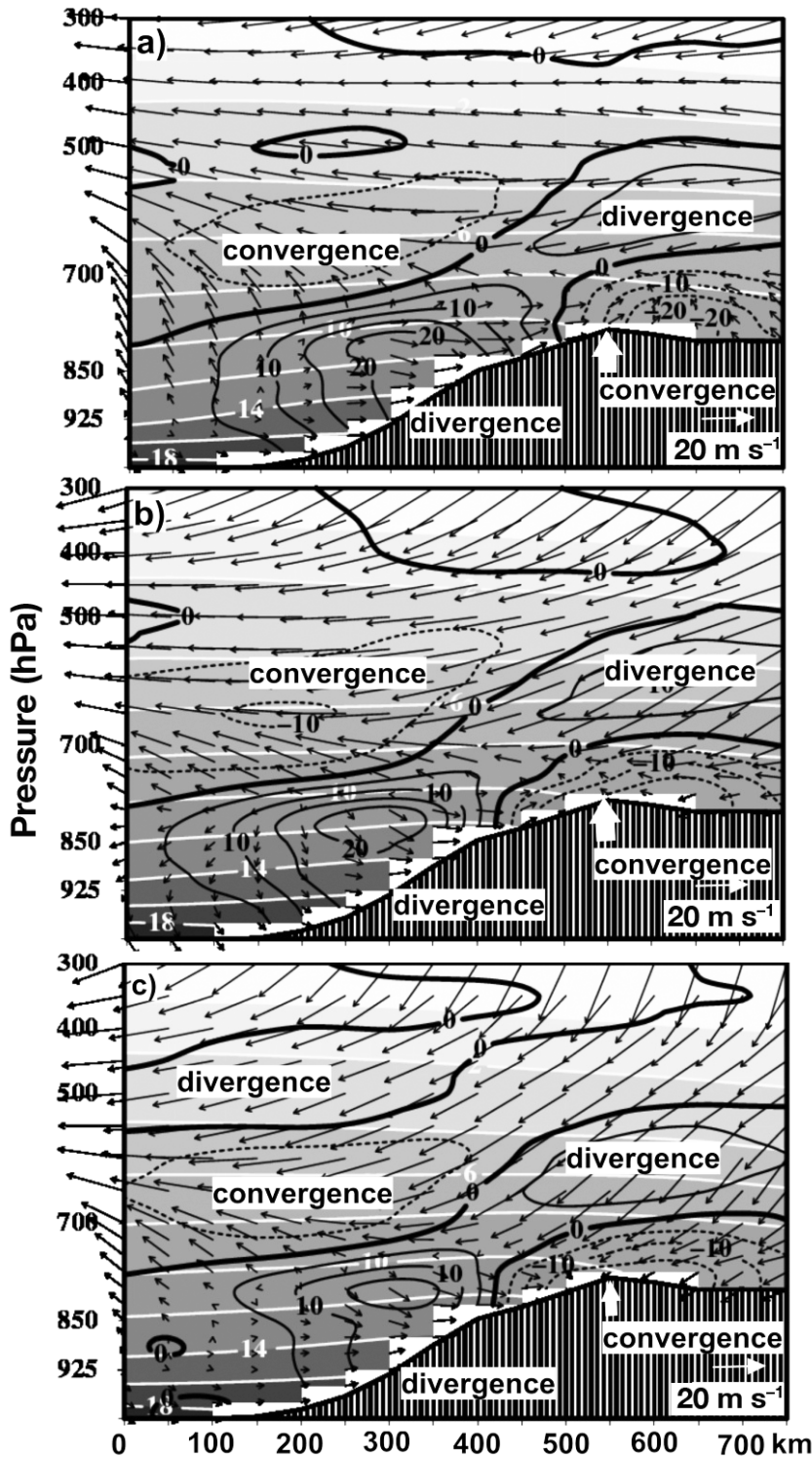


Fig. 12. Cross sections, 1000 hPa–300 hPa, from the NARR analyses for (a) July, (b) August, and (c) September 2015. The section is from 106.0° W, 21.2° N through 103.7° W, 24.8° N, across the San Pedro-Mezquital basin from southwest to northeast, as depicted in Fig. 1. Fields include average horizontal wind vectors, specific humidity (white lines, g kg^{-1}), divergence (black solid lines, 10^{-6} s^{-1}), and convergence (black dashed lines, 10^{-6} s^{-1}). White arrows represent the continental divide into the Altiplano, while the terrain profile is given by vertical lines

ico, while the rest of the country remained below the average. One synoptic-scale rainfall source was a low-pressure feature and its interaction with moisture from the Pacific. Tropical waves passing into the country moved rapidly, leaving little rainfall on the coast but higher than average rainfall in the interior of the continent. Records from Las Vegas indicate rainfall above average, in contrast to Acaponeta, where the July accumulation was below the corresponding average.

In August, below-average rainfall occurred at the coast and inland, in agreement with the national average (CONAGUA 2015). According to official reports, August 2015 was ranked as the tenth-driest August since 1941 nationwide.

In September, there were 5 states that had rainfall above the average, including Nayarit. It was the seventh-rainiest month since 1941, and 11 September was as the rainiest day of the month, with rainfall estimated at the national level at 8.7 mm, 4.4 mm more than the average for that day (1971–2000). According to official reports, weather systems that caused the September rains involved interactions of moisture from the Pacific and Atlantic coasts with 2 low-pressure areas. One covered northeastern, central, and southern Mexico and the other extended from Sonora to Jalisco. September was the wettest month in the coastal region compared to the drier July and August, while September was dry in the interior. In contrast, July was wet in the Mexican Altiplano but dry along the coast. Overall, the 2015 summer was ranked as the fifth-driest nationwide within the 1941–2015 period. Vega-Camarena et al. (2018) described the link between the occurrence of droughts and different combinations of El Niño Southern Oscillation, Pacific Decadal Oscillation (PDO), and Atlantic Multidecadal Oscillation (AMO) in the Mexican Altiplano. Several studies showed that

these climatic indices have great influence over the rainfall conditions in this region (Méndez & Magaña 2010, Martínez-Sánchez & Cavazos 2014, Vega-Camarena et al. 2018). For example, droughts are common when La Niña combines with opposite phases of the PDO and AMO, as occurred during the most severe (2011) and the most persistent (1998–2000) droughts, when La Niña combined with a negative phase of the PDO and a positive phase of AMO (Vega-Camarena et al. 2018). Moderate droughts occurred under the transition from El Niño to La Niña (or vice versa), regardless of whether the PDO and AMO were in phase or not. The combination of the strong 1982–1983 El Niño and out-of-phase PDO and AMO coincided with the moderate 1982–1983 drought in the Altiplano. However, in this case the link was classified as unusual. The occurrence of El Niño is particularly important to consider because of its link to the radiative feedback mechanism proposed by Ramanathan & Collins (1991), which has global implications. In our study, we postulate that the causes of drought in 2015 are mostly related to the deficits in rains that were observed in August.

According to Howard & Maddox (1988), MCSs in the coastal region of Nayarit and southern Sinaloa occur during July and August. However, in the summer of 2015, the convective activity was anomalous because MCSs were more frequent in September; this is contrasted by the precipitation deficit occurring in July and August. At the coast, this pattern resembles a midsummer drought flanked by 2 maxima, in July and September, with a minimum in August. Given that MCSs persist for more than 12 h, they are likely to have substantial impacts on agricultural and other economic activities. In other seasons, Acapometla had a rainfall pattern resembling the 2015 midsummer droughts of 1978, 2000, and 2002. These seasons had a wet September, along with increased formation of MCSs.

The midsummer drought is not a climate feature in regions dominated by monsoon circulations and, at the coast of Nayarit, it is caused by a different mechanism than in southern Mexico, Central America, and the Caribbean (Small et al. 2007, Karnauskas et al. 2013). Here, the midsummer drought is caused by a delay in MCS formation because, instead of a higher frequency in August, as suggested by the mean precipitation from 1951–2010, the actual period of more organized convection starts in September.

The dynamics of air flow in the San Pedro-Mezquital river basin suggest a relationship between low-level winds and rainfall. In the morning, when

flow with a southerly component dominates, there is heavy rainfall. During the evening, when there are winds with a northerly component, there is little to no rainfall. This is consistent with the moisture content above the ground, since northern winds are generally cold and dry in the morning, while winds from the south advect more moisture off the coast, and therefore, favor a more humid environment for the development of deep convection over mountainous terrain. This process generates rainfall over the mountains during the day, which moves to the coast during the evening.

When winds, coming from the north, strengthen in the interior of the continent, the weather is dry. This suggests that moisture is transported from the coast to the interior by winds from the southwest. During the day, when moist air meets the winds from the north (northeast or northwest) that are relatively cold and dry, the moisture condenses into fog banks that do not produce rain. We frequently observed fog banks in the field (Fig. S3 in the Supplement), mainly in the morning, and especially extensive in the canyons of the San Pedro-Mezquital river system, causing dry and clear weather the rest of the day.

5. CONCLUSIONS

For the region between the coast of Nayarit and the Mexican Altiplano, a seesaw behavior in rainfall, with relatively dry conditions on the continent and more rainfall along the coast and vice versa, occurred during the summer of 2015. A similar condition occurred in 2000 and 2002. This behavior resembles the midsummer drought in southern Mexico and Central America. The mechanism causing this behavior originates from the gap in the occurrence of MCSs. That is, there are environmental conditions that provide more convection and enhanced rainfall in September over the coastal areas.

Some of the moisture from the eastern Pacific coast is advected into the continent, affecting portions of Nayarit, Durango, and Zacatecas. Between Nayarit and the Mexican Altiplano, there is a seesaw behavior, primarily due to intense and severe drought conditions (Vega-Camarena et al. 2018). The 2 regions are connected by the San Pedro-Mezquital river drainage basin, implying that rainfall is favored by southerly winds that advect low-level moisture from the Pacific to the higher elevations, as suggested by Brito-Castillo et al. (2010). The basin divide makes a large excursion inland, away from the coast and away from the bulk of the Sierra Madre Occidental

massif. As such, the elevation of the basin divide (and continental divide) is lower than in other regions of the Sierra Madre Occidental. The displacement, combined with a relatively low elevation, appears to allow significant penetration of moisture into the continent.

Part of the humid air rises due to the canyon pathways in the mountainous terrain, causing orographic precipitation during the day and nocturnal rainfall along coastal areas. If the northerly winds, relatively cold and dry, intensify over the continent, moisture coming from south condenses near the surface to form fog banks that produce no rain.

Acknowledgements. This project was funded by CIBNOR (grant PPAC-PC 0.3) and REDESClim-CONACYT (grant 254533). J.P.V.C. is the recipient of a doctoral fellowship from CONACYT (grant 376783). The authors thank the anonymous reviewers for comments that improved the manuscript. This study is dedicated to the memory of Ira Fogel (1935–2018), who edited this manuscript. We learned so much from each interaction; his enthusiasm and dedication to science will be missed.

LITERATURE CITED

- ✦ Berbery EH (2001) Mesoscale moisture analysis of the North American Monsoon. *J Clim* 14:121–137
- ✦ Brito-Castillo L, Vivoni ER, Gochis DJ, Filonov A, Tereshchenko I, Monzon C (2010) An anomaly in the occurrence of the month of maximum precipitation distribution in northwest Mexico. *J Arid Environ* 74:531–539
- CENAPRED (Centro Nacional de Prevención de Desastres) (2014) Atlas climatológico de ciclones tropicales en México. www.cenapred.gob.mx/es/Publicaciones/archivos/37.pdf
- CONAGUA (Comisión Nacional del Agua) (2015) Reporte anual del clima en México 2015. <https://smn1.conagua.gob.mx/climatologia/analisis/reporte/Anual2015.pdf>
- CONANP (Comisión Nacional de Áreas Naturales Protegidas) (2013) Fichas de evaluación ecológica de áreas naturales protegidas del noroeste de México. https://simec.conanp.gob.mx/pdf_score/16.pdf
- ✦ Farfán LM, Zehnder JA (1994) Moving and stationary mesoscale convective systems over northwest Mexico during the Southwest Area Monsoon Project. *Weather Forecast* 9:630–639
- ✦ Farfán LM, Alfaro EJ, Cavazos T (2013) Characteristics of tropical cyclones making landfall on the Pacific coast of Mexico: 1970–2010. *Atmósfera* 26:163–182
- ✦ Giovannetone JP, Barros AP (2008) A remote sensing survey of the role of landform on the organization of orographic precipitation in Central and Southern Mexico. *J Hydrometeorol* 9:1267–1283
- ✦ Gochis DJ, Jimenez A, Watts CJ, Garatuza-Payan J, Shuttleworth WJ (2004) Analysis of 2002 and 2003 warm-season precipitation from the North American Monsoon Experiment Event Rain Gauge Network. *Mon Weather Rev* 132: 2938–2953
- ✦ Higgins W, Gochis D (2007) Synthesis of results from the North American monsoon experiment (NAME) process study. *J Clim* 20:1601–1607
- Higgins RW, Douglas AV, Hahmann A, Berbery EH and others (2003) Progress in Pan American CLIVAR Research: the North American Monsoon system. *Atmósfera* 16: 29–65
- Houze RA Jr (1993) *Cloud Dynamics*. Academic Press, San Diego, CA
- Howard KW, Maddox RA (1988) Mexican mesoscale convective systems—a satellite perspective. *Proc Third Inter-American and Mexican Congress of Meteorology*. Mexican Meteorological Organization, Mexico City, p 404–408
- ✦ Kalnay E, Kanamitsu M, Kistler R, Collins W and others (1996) The NCEP/NCAR 40-year reanalysis project. *Bull Am Meteorol Soc* 77:437–471
- ✦ Karnauskas KB, Seager R, Giannini A, Busalacchi AJ (2013) A simple mechanism for the climatological midsummer drought along the Pacific coast of Central America. *Atmósfera* 26:261–281
- ✦ Ladwig WC, Stensrud DJ (2009) Relationship between tropical easterly waves and precipitation during the North American monsoon experiment. *J Clim* 20:257–271
- ✦ Magaña V, Amador JA, Medina S (1999) The midsummer drought over Mexico and Central America. *J Clim* 12: 1577–1588
- ✦ Martínez-Sánchez JN, Cavazos T (2014) Eastern Tropical Pacific hurricane variability and landfalls on Mexican coasts. *Clim Res* 58:221–234
- McKee TB, Doeskin NJ, Kleist J (1993). The relationship of drought frequency and duration to time scales. *Proceedings of the Eighth Conference on Applied Climatology*. American Meteorological Society, Anaheim, CA, p 179–184
- ✦ Méndez M, Magaña V (2010) Regional aspects of prolonged meteorological droughts over Mexico and Central America. *J Clim* 23:1175–1188
- ✦ Mesinger F, DiMego G, Kalnay E, Mitchell K and others (2006) North American regional reanalysis. *Bull Am Meteorol Soc* 87:343–360
- Mosiño PA, García E (1974) The climate of Mexico. In: Bryson RA, Hare FK (eds) *World survey of climatology, Vol 2: climates of North America*. Elsevier, London, 345–404
- ✦ North GR, Bell TL, Cahalan RF, Moeng FJ (1982) Sampling errors in the estimation of empirical orthogonal functions. *Mon Weather Rev* 110:699–706
- ✦ Purdom JFW (1976) Some uses of high-resolution GOES imagery in the mesoscale forecasting of convection and its behavior. *Mon Weather Rev* 104:1474–1483
- ✦ Ramanathan V, Collins W (1991) Thermodynamic regulation of ocean warming by cirrus clouds deduced from observations of the 1987 El Niño. *Nature* 351:27–32
- Ropelewski CF, Gutzler DS, Higgins RW, Mechoso CR (2005) The North American monsoon system. In: Chang CP, Wang B, Lau NCG (eds) *The global monsoon system: research and forecast*. World Meteorological Organization, Geneva, p 207–218
- ✦ Small RJO, De Szoeke SP, Xie SP (2007) The Central American midsummer drought: regional aspects and large-scale forcing. *J Clim* 20:4853–4873
- ✦ Turrent C, Cavazos T (2009) Role of the land-sea thermal contrast in the interannual modulation of the North American Monsoon. *Geophys Res Lett* 36:L02808
- Valdés-Manzanilla A, Cortéz-Vázquez M, Pastrana-Fran-

- cisco JJ (2005) Un estudio explorativo de los sistemas convectivos de mesoescala de México. *Invest Geogr* 56:26–42
- ✦ Vega-Camarena JP, Brito-Castillo L, Farfán LM, Gochis DJ, Pineda-Martínez LF, Díaz SC (2018) Ocean-atmosphere conditions related to severe and persistent droughts in the Mexican Altiplano. *Int J Climatol* 38:853–866
- ✦ Velasco I, Fritsch JM (1987) Mesoscale convective complexes in the Americas. *J Geophys Res Atmos* 92:9591–9613
- Zillman J (2009) A history of climate activities. *WMO Bulletin* 58:141–150
- Zipser EJ (1982) Use of a conceptual model of the life-cycle of mesoscale convective systems to improve very-short-range forecasts. In: Browning KA (ed) *Nowcasting*. Academic Press, London, p 191–204

*Editorial responsibility: Ricardo Trigo,
Lisbon, Portugal*

*Submitted: November 22, 2017; Accepted: September 5, 2018
Proofs received from author(s): October 21, 2018*